International Journal of Dynamics and Control
https://doi.org/10.1007/s40435-019-00513-0

On the dynamics of a kicked harmonic oscillator

J. M. Tuwankotta[1] · **A. F. Ihsan**[1]

Received: 3 July 2018 / Revised: 29 December 2018 / Accepted: 22 January 2019

Abstract
In this paper the dynamics of a kicked harmonic oscillator is studied. This is done by constructing a stroboscopic map for the kicked harmonic oscillator by following the time t-flow of the differential equation and taking phase portrait for some integrals multiple of the period of the kicked. The resulting map is a two-dimensional area-preserving (or symplectic) map. We provide a proof for the continuity of the position, and also a local stability analysis for the trivial equilibrium. Complete analysis for a general kick function for the 1:1, and for the 1:2 resonances are presented. For the 1:4 resonance, we describe the dynamics numerically for some specific kick functions.

Keywords Area-preserving map · Dynamics · Resonance

1 Introduction

The dynamics of a two dimensional area-preserving (or symplectic) map is a very interesting classical subject that has been studied extensively in the literature (see for example in [1–4]). One of the key results is the existence of quasi-periodic motions on invariant curves in the neighbourhood of an elliptic fixed point. However, complicated dynamics. e.g. a more complex invariant structure or even chaos, might still be present between those invariant curves (see [5, 6]). See also [7] for a discussion on an extension to higher dimensional problem.

Consider a one degree of freedom nonautonomous Hamiltonian system. One might define a Poincaré map by following a time T-flow of a one degree of freedom, nonautonomous, Hamiltonian system of ordinary differential equations for some fixed T. This is also known as the stroboscopic map. The resulting map is a two-dimensional area-preserving map.

Let us now consider a two degrees of freedom Hamiltonian system. Let us fix a regular value for the Hamiltonian function. The level set of the Hamiltonian function for that regular value is a three dimensional manifold. Now, consider a two-dimensional section which is transversal (at least locally) to the flow. Then, starting from an arbitrary point on that previously chosen section as initial condition, we follow the flow of the Hamiltonian system until it comes back to the section while preserving the direction of velocity vector at the intersection. By this we have defined a mapping from the section to it self by following the flow. This Poincaré map is a two-dimensional area-preserving map.

In practise, it is not easy to construct an analytical expression for those Poincaré maps. Then, one might try to use a numerical method to integrate the Hamiltonian vector field, and thus, constructing the Poincaré map numerically. Another way is by using perturbation methods, such as normal form theory or averaging method, to construct an approximate system which Poincaré map is easier to construct analytically. See [8–10] and the references therein.

As an example, in [11] a numerical Poincaré map is constructed for a two degrees of freedom Hamiltonian mechanical system, i.e. the so-called elastic pendulum. When dealing with higher order resonance, the numerical integration has to be done for a rather long period of integration time. In [12], a geometric integration method is applied to derive a relatively accurate result in a rather short computational time.

Another example is the celebrated Hénon map [3]. This map is derived as an approximation for a Poincaré section of the three dimensional ordinary differential equations called the Lorenz model [13].

This research is supported by Riset P3MI 2017, Institut Teknologi Bandung, Indonesia.

✉ J. M. Tuwankotta
theo@math.itb.ac.id

[1] Analysis and Geometry, FMIPA, Institut Teknologi Bandung, Ganesha no 10, Bandung, Indonesia

Published online: 01 February 2019

A kicked harmonic oscillator is in a sense a special example where analytical expression for the stroboscopic map can be derived. Zaslavskii et al in [14] derived a two dimensional area-preserving map from a kicked harmonic oscillator. In [15] a similar two-dimensional map is considered. A phenomena called *tiling* (where the phase portrait of the map is a periodic copies of a small part of it) is described. Similar situation can be found in [16]. A different approach is used in [17] to describe a dynamical properties of the Harmonic kicked oscillators.

In applications, a kicked harmonic oscillator serves as a model for electronic transport in semiconductor superlattices [18] and atom optic modelling using ion-traps [19]. A similar system is analyzed in [20–25] to study the relation between classical and quantum dynamics. Variations of the model is also considered, for example by introducing damping into the system [26] or a coupled system consisting of kicked harmonic oscillations [27].

In this paper we consider a two dimensional area-preserving map derived from a kicked harmonic oscillator. The traditional approach in the literature is to assume continuity of the position of the oscillator and allows the velocity to have a jump discontinuity. This is a reasonable assumption from the physics point of view. Here we prove the continuity of the position under a rather general condition.

We are interested in particular for the case where the linear part of the mapping is a linear rotation with the angle of 0, π, and $\frac{\pi}{2}$. This rotation angles are related to the 1:1-, 1:2- and 1:4- resonances. A complete description of the dynamics for the first two cases can be done for any continuous function f while the latter is done numerically for three specific functions.

2 Problem formulation

A kicked harmonic oscillator is a second order differential equation which is defined by

$$\ddot{x} + {\omega_0}^2 x = R_0 f(x) \sum_1^\infty \delta_0(t - nT), \tag{1}$$

where $\omega_0, R_0, T \in \mathbb{R}^+$. The parameter ω_0 is the natural frequency of the oscillator. The parameters R_0 and T are called the amplitude and the period of the kick, respectively. We assume that the function f is continuous with $f(0) = 0$ and δ_0 is the dirac function with the property: $\delta_0(x)$ vanishes for every $x \neq 0$, and

$$\int_{\mathbb{R}} g(t)\delta_0(t)dt = g(0),$$

for any function g.

For $t \in [(k-1)T, kT)$, the oscillator (1) is a linear oscillator with solution:

$$x(t) = A_k \cos\omega_0 t + B_k \sin\omega_0 t, \tag{2}$$

$$\dot{x}(t) = -\omega_0 A_k \sin\omega_0 t + \omega_0 B_k \cos\omega_0 t, \tag{3}$$

where A_k and B_k are constant, $k = 1, 2, 3, \ldots$.

Continuity of the position Note that we have:

$$\dot{x}(kT+\varepsilon) - \dot{x}(kT-\varepsilon) = \int_{kT-\varepsilon}^{kT+\varepsilon} \ddot{x}(s)ds,$$

for a fixed $k = 1, 2, 3, \ldots$. From Eq. (1), we derive:

$$\begin{aligned}\dot{x}(kT+\varepsilon) - \dot{x}(kT-\varepsilon) = &-\int_{kT-\varepsilon}^{kT+\varepsilon} x(s)ds \\ &+ \int_{kT-\varepsilon}^{kT+\varepsilon} R_0 f(x(s)) \sum_1^\infty \delta_0(s-nT)ds.\end{aligned} \tag{4}$$

Let us consider the following lemma.

Lemma 1 *Let $\varphi : (a-t_0, a+t_0) \longrightarrow \mathbb{R}$, where $a \in \mathbb{R}$ and $t_0 > 0$. We assume that:*

$$\lim_{t\to a^-} \varphi(t) = L < \infty \text{ and } \lim_{t\to a^+} \varphi(t) = K < \infty$$

for some L and K in $\mathbb{R}$. Then:

$$\lim_{t_0\to 0^+} \int_{a-t_0}^{a+t_0} \varphi(s)ds = 0.$$

Proof Since $\lim_{t\to a^-} \varphi(t) = L$ then, there exists $\delta_1 > 0$ such that: if $0 < a - t < \delta_1$ then

$$L - 1 < \varphi(t) < L + 1.$$

Since $\lim_{t\to a^-} \varphi(t) = K$ then, there exists $\delta_2 > 0$ such that: if $0 < t - a < \delta_2$ then

$$K - 1 < \varphi(t) < K + 1.$$

Thus, for every t such that $0 < |t-a| < \delta = \min\{\delta_1, \delta_2\}$, we have:

$$m = \min\{L-1, K-1\} < \varphi(t) < \max\{L+1, K+1\} = M.$$

As a consequence, for every $0 < t_0 < \delta$, we derive:

$$2mt_0 \le \int_{a-t_0}^{a+t_0} \varphi(s)ds \le 2Mt_0,$$

which goes to zero as $t_0 \to 0$. □

It is clear that $x(t)$ satisfies the condition in Lemma 1 for $t \in (kT-\varepsilon, kT+\varepsilon)$. As a consequence, we have:

$$\lim_{\varepsilon\to 0} \int_{kT-\varepsilon}^{kT+\varepsilon} x(s)ds = 0.$$

From (3) we know that the velocity $\dot{x}$ is continuous on $[(k-1)T, kT)$ with at most a jump-discontinuity at $t = kT$, for all $k = 1, 2, \ldots$, and furthermore, that $\dot{x}(t)$ is bounded on every closed interval.

Proposition 1 *The solution $x(t)$ of (1) is a continuous function of t.*

Proof Let ε be an arbitrary positive small number. For a fixed k in $\{0, 1, 2, 3, \ldots\}$, let M_k and m_k be the maximum and the minimum of $\dot{x}$ on the interval $[kT - \frac{1}{2}T, kT + \frac{1}{2}T]$, respectively. Then:

$$2m_k\varepsilon \le \int_{kT-\varepsilon}^{kT+\varepsilon} \dot{x}(x)ds \le 2M_k\varepsilon,$$

which implies that:

$$\lim_{\varepsilon\to 0} x(kT+\varepsilon) - x(kt-\varepsilon) = 0.$$

□

Derivation of the Poincaré map We proceed with deriving a two-dimensional mapping by following the time T flow of the solution of (1). This map is also known as the *strobocospic* map or the Poincaré map for (1).

Let us define:

$$\begin{aligned} x_k &= A_k \cos\omega_0 kT + B_k \sin\omega_0 kT, \\ \dot{x}_k &= -A_k\omega_0 \sin\omega_0 kT + B_k\omega_0 \cos\omega_0 kT. \end{aligned} \tag{5}$$

Let us fix a value for k in $\{1, 2, \ldots\}$. Substituting (3) to (4), and then taking $\varepsilon \to 0$, we derive:

$$\begin{aligned} &-\big(A_{k+1} - A_k\big)\sin\omega_0 kT + \big(B_{k+1} - B_k\big)\cos\omega_0 kT \\ &\quad = \tfrac{1}{\omega_0} f(x_k). \end{aligned} \tag{6}$$

Furthermore, from Proposition (1) we derive:

$$\big(A_{k+1} - A_k\big)\cos\omega_0 kT + \big(B_{k+1} - B_k\big)\sin\omega_0 kT = 0. \tag{7}$$

Solving (6) and (7) we derive:

$$\begin{aligned} A_{k+1} &= A_k - \tfrac{1}{\omega_0} R_0 f(x_k)\sin\omega_0 kT \\ B_{k+1} &= B_k + \tfrac{1}{\omega_0} R_0 f(x_k)\cos\omega_0 kT \end{aligned} \tag{8}$$

Substituting (8) into (5) we derive:

$$\begin{aligned} x_{k+1} &= \Big(A_k - \tfrac{1}{\omega_0} R_0 f(x_k)\sin\omega_0 kT\Big) \\ &\qquad \big(\cos\omega_0 kT\cos\omega_0 T - \sin\omega_0 kT\sin\omega_0 T\big) \\ &\quad + \Big(B_k + \tfrac{1}{\omega_0} R_0 f(x_k)\cos\omega_0 kT\Big) \\ &\qquad \big(\sin\omega_0 kT\cos\omega_0 T + \cos\omega_0 kT\sin\omega_0 T\big) \\ &= x_k\cos\omega_0 T + \tfrac{1}{\omega_0}\big(\dot{x}_k + R_0 f(x_k)\big)\sin\omega_0 t. \end{aligned}$$

Similarly, we can derive the equation for $\dot{x}_{k+1}$, and thus, we have a two-dimensional mapping:

$$\begin{pmatrix} x_{k+1} \\ \dot{x}_{k+1} \end{pmatrix} = \begin{pmatrix} \cos\omega_0 T & \frac{1}{\omega_0}\sin\omega_0 T \\ -\omega_0\sin\omega_0 T & \cos\omega_0 T \end{pmatrix} \begin{pmatrix} x_k \\ \dot{x}_k + R_0 f(x_k) \end{pmatrix}.$$

Let us now rescale the variable by: $\dot{x}_k = \omega_0 y_k$, and the parameter by: $R_0 = R\omega_0$, and $\omega_0 T = \theta$. Then, we derive:

$$\begin{pmatrix} x_{k+1} \\ y_{k+1} \end{pmatrix} = \mathrm{rot}(\theta)\begin{pmatrix} x_k \\ y_k + Rf(x_k) \end{pmatrix},$$

where

$$\mathrm{rot}(\theta) = \begin{pmatrix} \cos\theta & \sin\theta \\ -\sin\theta & \cos\theta \end{pmatrix}.$$

This mapping is similar to the one in [14, 15] with the function $f(x) = \sin x$ or with the mapping in [16] where f is taken as the sawtooth (piecewise-linear) function.

For our purpose, it is convenient to separate the linear rotation from the two-dimensional map. For this we define:

$$\begin{pmatrix} u_k \\ v_k \end{pmatrix} = \mathrm{rot}(-\theta)\begin{pmatrix} x_k \\ y_k \end{pmatrix}.$$

Then:

$$\begin{pmatrix} u_{k+1} \\ v_{k+1} \end{pmatrix} = \mathrm{rot}(\theta)\begin{pmatrix} u_k \\ v_k \end{pmatrix} + \begin{pmatrix} 0 \\ Rf(u_k\cos\theta + v_k\sin\theta) \end{pmatrix}, \tag{9}$$

where $R \in \mathbb{R}, \theta \in (-\pi, \pi]$.

3 Dynamical properties of (9) for general f

Let us start with exploring the properties of the mapping (9) for general function f. Since we have assumed that $f(0)$ is zero, then $(u, v) = (0, 0)$ is an equilibrium.

The Area-preserving nature of the map (9) Let us assume that, $f : \mathbb{R} \longrightarrow \mathbb{R}$ has Taylor expansion in the neighborhood of $x = 0$, with non-vanishing first derivative. Furthermore, let us define

$$g(x) = f(x) - \frac{df}{dx}(0)x.$$

Without loss of generality, we assume that $\frac{df}{dx}(0) = 1$, since this can be arranged by rescaling R and the function g. Then the map (9) can written as:

$$\begin{pmatrix} u' \\ v' \end{pmatrix} = A(R,\theta)\begin{pmatrix} u \\ v \end{pmatrix} + R\begin{pmatrix} 0 \\ g(u\cos\theta + v\sin\theta) \end{pmatrix}, \qquad (10)$$

with

$$A(R,\theta) = \begin{pmatrix} \cos(\theta) & \sin(\theta) \\ -\sin(\theta) + R\cos(\theta) & \cos(\theta) + R\sin(\theta) \end{pmatrix}.$$

Since $\det(A(R,\theta)) = 1$ then the mapping (9) is *area preserving*.

Remark 1 The area preserving nature of the mapping (9) can also be derived from the fact that the system (1) is a Hamiltonian system with Hamiltonian:

$$H(x,y) = \frac{1}{2}y^2 + \frac{1}{2}{\omega_0}^2x^2 - F(x)\sum_1^\infty \delta_0(t - nT),$$

with $F'(x) = R_0 f(x)$. See [17].

Stability of the trivial fixed point Let us look at the characteristic polynomial of $A(R,\theta)$, i.e.

$$p(\lambda) = \lambda^2 - (2\cos(\theta) + R\sin(\theta))\lambda + 1.$$

The eigenvalues of the Jacobian of (9) in the vicinity of the origin can be written as:

$$\lambda_{1,2} = \alpha(R,\theta) \pm \mathrm{i}\sqrt{1 - (\alpha(\theta,R))^2}, \qquad (11)$$

with:

$$\alpha(R,\theta) = \cos(\theta) + \frac{R}{2}\sin(\theta).$$

For $R = 0$, the eigenvalues are: $\cos\theta \pm \mathrm{i}\sin\theta$. Note that $\frac{d}{dR}\alpha(R,\theta)$ is sign definite for fixed θ, which implies that α is a monotonic function with respect to R. These eigenvalues collide with each other at $\lambda = 1$, for

$$R = \frac{2 - 2\cos(\theta)}{\sin(\theta)},$$

and at $\lambda = -1$, for

$$R = -\frac{2 + 2\cos(\theta)}{\sin(\theta)}.$$

Analyzing the eigenvalues $\lambda_{1,2}$ in (11) we derive the stability type of the trivial fixed point of (9) which depends on two parameter R and θ. The result is presented in Fig. 1.

For each $\theta \notin \{0, -\pi\}$, there exists an interval I containing 0, such that the trivial fixed point is elliptic for $R \in I$. Combining this with the area preserving nature of (9) we derive that there exists a continuous family of closed curves surrounding the origin which are invariant with respect to (9). We note that the length of the interval I becomes larger as θ approaches $\frac{\pi}{2}$ from the left, or $-\frac{\pi}{2}$ from the right. For $\theta = 0$ or $-\pi$, the trivial fixed point is of parabolic type.

Weakly nonlinear case As for the stability of the trivial equilibrium, the case where the derivative of f at $x = 0$ vanishes can be seen as the case where $R = 0$ in the stability diagram in Fig. 1. Then the eigenvalues for $A(\theta, R)$ are:

$$\lambda_{1,2} = \cos\theta \pm \mathrm{i}\sin\theta.$$

This implies that the trivial fixed point is either: elliptic when $\theta \notin \{0, \pi\}$ or parabolic when $\theta \in \{0, \pi\}$. Thus, varying the value of R does not change the stability type of the trivial equilibrium. If $f'(0) = 1$, if one would like to have a linear rotation with an angle θ_0, then one would have top choose R and θ such that:

$$\cos\theta_0 = \cos\theta + \frac{R}{2}\sin\theta,$$

$$\text{if } -1 < \cos\theta + \tfrac{R}{2}\sin\theta < 1.$$

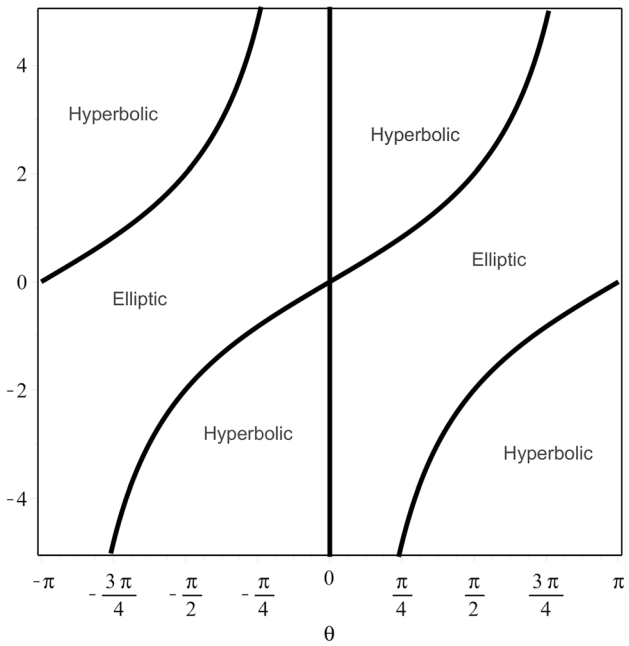

Fig. 1 Stability type domain in parameter space (θ, R) of the trivial fixed point of the map (9) for $f'(0) = 1$. Apart from the curve, we note that the $\theta = 0$ line is also a boundary set where the trivial fixed point is of parabolic type

On resonance In particular, we are interested on studying the dynamics of (9) for: $\theta = 0, \pi$ and $\theta \approx \frac{\pi}{2}$. Recall that we have defined: $\theta = \omega_0 T$. Let us now write: $\omega_k = \frac{2\pi}{T}$ which is the frequency of the kick. Then:

$$\theta = \omega_0 \frac{2\pi}{\omega_k} \text{ or, equivalently: } \frac{\theta}{2\pi} = \frac{\omega_0}{\omega_k}.$$

Thus, $\theta = 0$ which can be seen as $\theta = 2\pi$, corresponds to the $\omega_0 : \omega_k = 1 : 1$. This is also known as the 1:1-resonance. Similarly, $\theta = \pi$ corresponds to the 1:2-resonance, while $\theta = \frac{\pi}{2}$ corresponds to the 1:4-resonance.

Linear growth Let us consider the case where $\theta = 0$. In this case the mapping (9) becomes:

$$\begin{pmatrix} u_{k+1} \\ v_{k+1} \end{pmatrix} = \begin{pmatrix} u_k \\ v_k \end{pmatrix} + R \begin{pmatrix} 0 \\ f(u_k) \end{pmatrix}, k = 0, 1, 2, \ldots .$$

It is clear that the phase space $\mathbb{R}^2$ is fibered by the vertical lines: $u = u_0$, $u_0 \in \mathbb{R}$. On each line, v linearly grows without bound with a fixed step of $\Delta v = Rf(u_0)$, whenever $f(u_0) > 0$, or decreases without bound with a fixed step of $\Delta v = -Rf(u_0)$ whenever $f(u_0) < 0$. If $f(u_0) = 0$, then the line is a line of fixed points. We summarize in the following proposition.

Proposition 2 *If $\theta = 0$ then for any $(u_0, v_0) \in \mathbb{R}^2$ the solution of (9), starting at (u_0, v_0) reads:*

$$\begin{pmatrix} u_n \\ v_n \end{pmatrix} = \begin{pmatrix} u_0 \\ v_0 + nRf(u_0) \end{pmatrix} \tag{12}$$

where $n \in \mathbb{N}$. If $f(u_0) = 0$ then every point (u_0, v), $v \in \mathbb{R}$ is fixed by the mapping (9), i.e. the line:

$$\ell = \{(u_0, v) \mid v \in \mathbb{R}\}$$

is a line of fixed points of (9).

Period-2 dynamics Let us now look at the case where $\theta = \pi$. In this case, the matrix $\text{rot}(\pi) = -I$. Since $(-I)^2 = I$ we would like to find some period-2 points in $\mathbb{R}^2$. The mapping (9) in this case, becomes:

$$\begin{pmatrix} u_{k+1} \\ v_{k+1} \end{pmatrix} = -\begin{pmatrix} u_k \\ v_k \end{pmatrix} + R \begin{pmatrix} 0 \\ f(u_k) \end{pmatrix}, k = 0, 1, 2, \ldots .$$

Thus, $u_n = (-1)^n u_0$ for $n = 1, 2, 3 \ldots$. An immediate consequence of this is the manifold:

$$\left\{ (u, v) \in \mathbb{R}^2 \;\middle|\; u = \pm u_0 \text{ for any fixed } u_0 \right\}$$

is invariant with respect to (9). We have the following proposition which is proved by induction.

Proposition 3 *For the case where $\theta = \pi$, the solution $(u_n, v_n)^T$ of (9) starting at $(u_0, v_0) \in \mathbb{R}^2$ reads: $u_n = (-1)^n u_0$, and $v_n =$*

$$\begin{cases} -v_0 + R\left(\left(\frac{n+1}{2}\right) f(u_0) - \left(\frac{n-1}{2}\right) f(-u_0)\right) & \text{if } n \text{ is odd,} \\ v_0 + R\left(-\left(\frac{n}{2}\right) f(u_0) + \left(\frac{n}{2}\right) f(-u_0)\right) & \text{if } n \text{ is even.} \end{cases} \tag{13}$$

Proof Clearly, v_1 satisfies the above written formula. Let n be an arbitrary odd number, and let us assume (13) for a fixed natural number n. Thus

$$\begin{pmatrix} u_n \\ v_n \end{pmatrix} = -\begin{pmatrix} u_0 \\ v_0 \end{pmatrix} + R \begin{pmatrix} 0 \\ \left(\frac{n+1}{2}\right) f(u_0) - \left(\frac{n-1}{2}\right) f(-u_0) \end{pmatrix},$$

Since n is odd then $n + 1$ is an even number. Thus:

$$\begin{aligned} \begin{pmatrix} u_{n+1} \\ v_{n+1} \end{pmatrix} &= -\begin{pmatrix} u_n \\ v_n \end{pmatrix} + R \begin{pmatrix} 0 \\ f(u_n) \end{pmatrix} \\ &= \begin{pmatrix} u_0 \\ v_0 \end{pmatrix} + R \begin{pmatrix} 0 \\ -\left(\frac{n+1}{2}\right) f(u_0) + \left(\frac{n-1}{2}\right) f(-u_0) \end{pmatrix} \\ &\quad + R \begin{pmatrix} 0 \\ f(-u_0) \end{pmatrix} \\ &= \begin{pmatrix} u_0 \\ v_0 \end{pmatrix} + R \begin{pmatrix} 0 \\ -\left(\frac{n+1}{2}\right) f(u_0) + \left(\frac{n+1}{2}\right) f(-u_0) \end{pmatrix} \end{aligned}$$

Similarly, it can be shown that for even number n then the formula in (13) is satisfied. □

Proposition 4 *Consider the mapping (9) for the case where $\theta = \pi$. If f is an even function, then all solution except the trivial one, is periodic-2 solution. If f is an odd function, then the manifold*

$$\{(u_0, v) \mid f(u_0) = 0\}$$

is a manifold of period-2 points. For function which is neither even nor odd, the manifold

$$(u_0, v), v \in \mathbb{R},$$

where u_0 is a solution for: $f(u_0) - f(-u_0) = 0$, consists of period-2 points.

Proof The proof is done by requiring: $v_0 = v_2$ (or $v_1 = v_3$) which leads to: $f(u_0) = f(-u_0)$. □

For example, if $f(u) = u^3 - u + 1$ (which is neither an odd nor an even function), then the line $u = \pm 1$ consists of period-2 points (since $f(1) = f(-1)$).

4 Dynamics for $\theta = \frac{\pi}{2}$

Let us consider the cases where: $\theta = \pm\frac{1}{2}\pi$. These two cases are related to each other by time-reversal symmetry, i.e.: the case where $\theta = -\frac{1}{2}\pi$ is similar to $\theta = \frac{1}{2}\pi$ but reversing the direction of the rotation. We will be discussing the positive case.

The rotation matrix in this case is:

$$\mathrm{rot}\left(\frac{1}{2}\pi\right) = J = \begin{pmatrix} 0 & 1 \\ -1 & 0 \end{pmatrix}.$$

This matrix satisfies: $J^2 = -I$, $J^3 = -J$, and $J^4 = I$. The mapping (9) can be written as:

$$\begin{cases} u_{k+1} &= v_k, \\ v_{k+1} &= -u_k + Rf(v_k) \end{cases} k = 0, 1, 2, \ldots . \tag{14}$$

For simplicity of the notation, we write: f_k for $f(v_k)$. The general formula for the solution for arbitrary initial condition (u_0, v_0) as a function of n and the initial condition, is not very clear. However, it is clear that for $R = 0$ the dynamics of (14) consists of period-4 dynamics for all initial condition. For this reason, we we will look for period-4 points instead.

Applying the mapping, for $k = 0, 1, 2$, and 3, we have:

$$\begin{aligned}
k = 0 \implies & \begin{cases} u_1 &= v_0 \\ v_1 &= -u_0 + Rf_0 \end{cases} \\
k = 1 \implies & \begin{cases} u_2 &= v_1 & &= -u_0 + Rf_0 \\ v_2 &= -u_1 + Rf_1 & &= -v_0 + Rf_1 \end{cases} \\
k = 2 \implies & \begin{cases} u_3 &= v_2 & &= -v_0 + Rf_1 \\ v_3 &= -u_2 + Rf_2 & &= u_0 + R\left(f_2 - f_0\right) \end{cases} \\
k = 3 \implies & \begin{cases} u_4 &= v_3 & &= u_0 + R\left(f_2 - f_0\right) \\ v_4 &= -u_3 + Rf_3 & &= v_0 + R\left(f_3 - f_1\right) \end{cases}
\end{aligned}$$

For period-4 points, we set: $f_0 = f_2$ and $f_1 = f_3$. Note that:

$$f_3 = f(v_3) = f(u_0 - Rf_0 + Rf_2) = f(u_0),$$

if $f_0 = f_2$ is satisfied. Then, the period-4 points are found by solving:

$$\begin{cases} f(-v_0 + Rf(u_0)) &= f(v_0) \\ f(-u_0 + Rf(v_0)) &= f(u_0). \end{cases} \tag{15}$$

A trivial example where (15) is satisfied is when f is a constant function. In that case, all solution is periodic with period-4. However, since we require that the function is continuous and $f(0) = 0$, then $f(x) = 0$ for all $x \in \mathbb{R}$. Thus, all solution is fixed point.

If f is one to one, the condition reduces to: $u_0 = \frac{1}{2}Rf(v_0)$ and $v_0 = \frac{1}{2}Rf(u_0)$, or equivalently:

$$u_0 = \frac{1}{2}Rf\left(\frac{1}{2}Rf(u_0)\right).$$

Another special case is, if f is an odd function such that there exists $p \neq 0$ such that: $f(p) = 0$, then

$$\{(p, p), (-p, p), (-p, -p), (p, -p)\}$$

are period-4 points.

Case study: $f(x) = \frac{1}{6}x^3$ The equation for period-4 points is:

$$u_0 - \frac{R^4}{2^7 3^3}{u_0}^9 = 0.$$

The non vanishing solution for that equation is $2\sqrt{\frac{3}{R}}$. Thus, we derive four special points, i.e.: $(u, v) = \left(u_0, u_0\right), \left(-u_0, u_0\right), \left(-u_0, -u_0\right)$, or $\left(u_0, -u_0\right)$. However, all of these points are fixed point. Thus, we have not period-4 points. For small value of R these points go away from the origin into the domain where the solution becomes unbounded.

Note that the function f in this case is unbounded. This implies that solution for large initial condition might become unbounded also. Furthermore, the large the amplitude of the kick R, the faster solution will get in to the domain where solutions become unbounded. This is the reason why in the numerical exploration we have done, the above described fixed points are not visible.

In Fig. 2 we have plotted the phase portraits of the mapping (14) for various initial conditions, and various values of R. For the upper left diagram, the value of R is 0.5 while for the upper right one is 1.5. It is quite remarkable that instead of a period-4 behaviour, in these diagrams in Fig. 2 we observe period-5 points. Some of these points appear as ten islands surrounded by chaotic orbits. Thus, there are four pairs of five period-5 points. This is clear from the diagram on the second row in Fig. 2. In those diagrams, the initial condition have been chosen so that it shows that the two neighbouring islands belong to a different pair of period-5 points. Note that between two neighbouring island one can find another two pairs of five period-5 points which are of saddle type. It is also remarkable that these period-5 points persists for a large value of R. However, their locations get closer to the origin as R becomes large. Further investigation is needed to check if these points goes to the origin as R goes to infinity or if they disappear through saddle node bifurcations.

Apart from the period-5 points, there are other periodic behaviour, i.e. period-9 points that appear for $R = 0.5$. These points also appear in the diagram for $R = 5$ but not in the diagram for $R = 1.5$. We suspect that this is due to the size of the islands surrounding the period-9 points is too small, so that the set of initial condition we have chosen to produce the diagram for $R = 1.5$ cannot capture these points.

It is interesting to note that inside the island of period-5 points, there are other high-period behaviour. See the

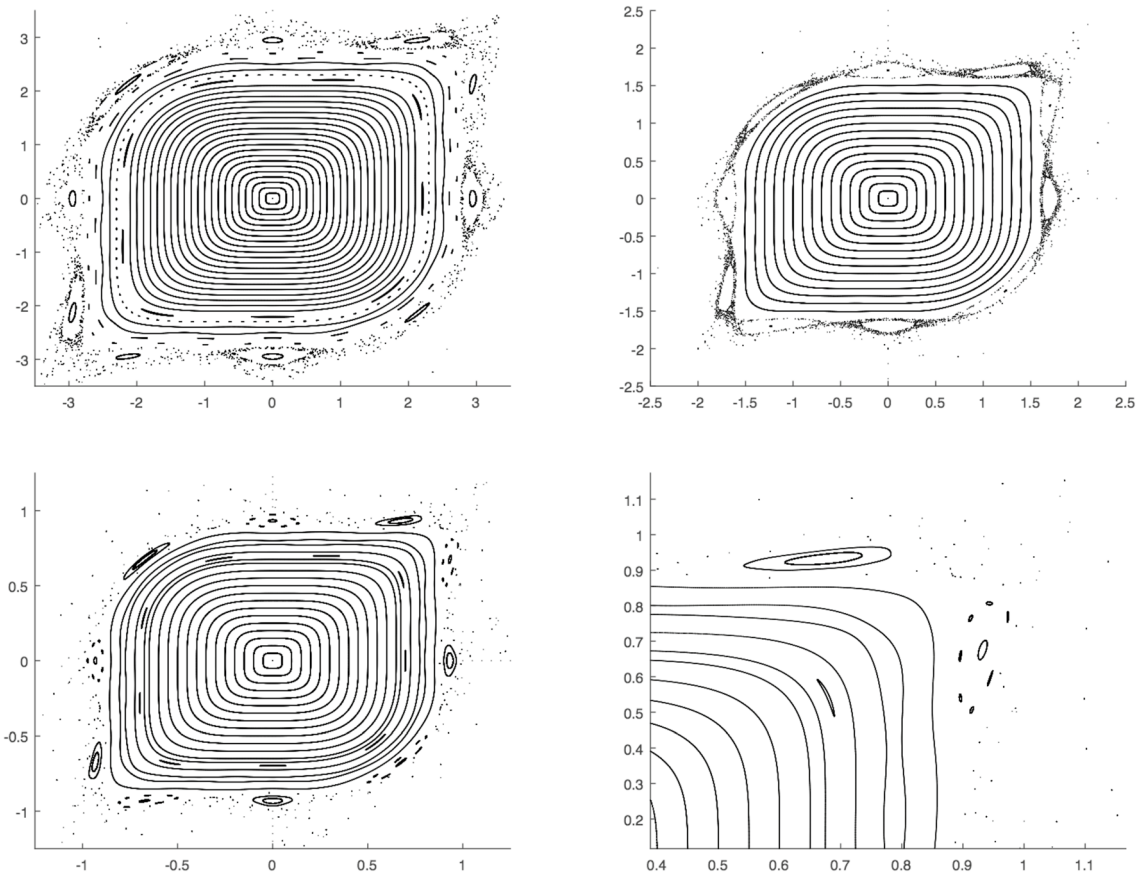

Fig. 2 In this figure we have plotted the dynamics of (14) for for various initial condition. For the left diagram in the first row, the value of $R = 0.5$, and for the diagram on the right 1.5. In the second row, the value of R is 5 for both diagrams

lower left diagram in Fig. 2. This behaviour is very clear in the diagram for $R = 5$. We have zoomed in the neighborhood $[0.4, 1.1] \times [0.1, 1.1]$ in the lower right diagram. In this diagram one can see the appearance of high-period periodic points inside the island of period-5 points.

Case study: $f(x) = x - \sin x$

Our next case study is for

$$f(x) = x - \sin x = \frac{1}{6}x^3 - \frac{1}{5!}x^5 + \dots .$$

In [15], the phenomena of tiling and existence of the so-called stochastic web, due to the periodic perturbation for the map (9), is described. In [16] similar phenomena is observed. In the latter the author there also consider a periodic perturbation of the map (14). It is interesting to note that the function f is not periodic. However, the tiling phenomena and the stochastic web are observed in the phase-portrait. See the left diagram in Fig. 3.

Since f is unbounded, for $R = 5$ then the tilling phenomena disappear. The dynamics of (9) remain bounded only inside $[-1, 1] \times [-1, 1]$. The four pairs of five period-5 points are still visible in the case where $R = 1$ and $R = 5$. Their locations are getting closer to the origin as R become large. This is a similar situation with the first case study where $f(x) = \frac{1}{6}x^3$. The main different between the first case study and the second is the appearance of the tilling phenomena. Further investigation is needed to understand the mechanism that produces this tilling phenomena since, both are non-periodic functions.

5 Concluding remark

In the paper we have studied a two dimensional map which is derived from a kicked harmonic oscillator. We have proved that under the assumption on f being continuous in the whole real line, then the position of the kicked harmonic oscillator is continuous with respect to time, while the velocity is piece-wise continuous with at most a jump discontinuity at every integral multiple of the period of the kicked.

For the case where $\theta = \frac{\pi}{2}$ (or the 1:4-resonance), we have chosen two functions as case studies for the kick function f, i.e. $f(x) = \frac{1}{6}x^3$, and $f(x) = x - \sin x$. It is easy

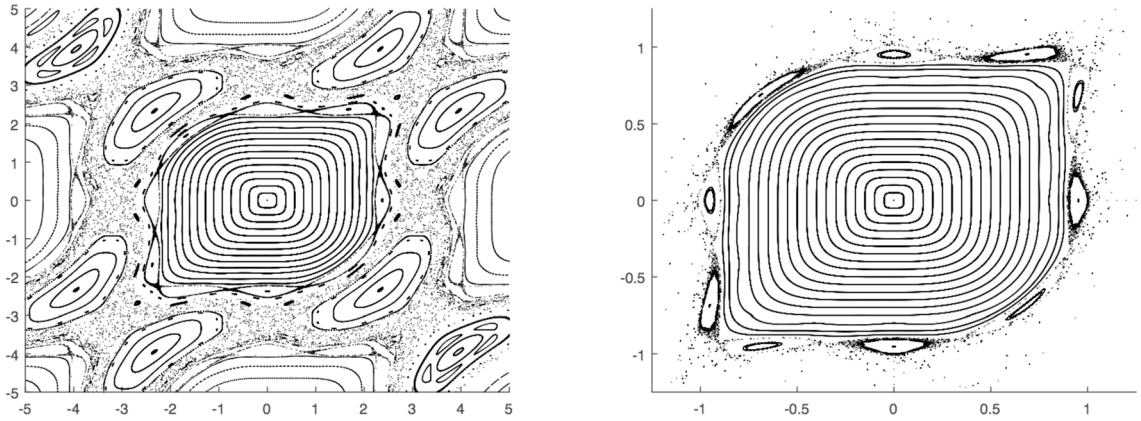

Fig. 3 The phase-portrait of (14) for $f(x) = x - \sin x$, and $R = 1$ (the left hand side diagram) and $R = 5$ the right hand side diagram)

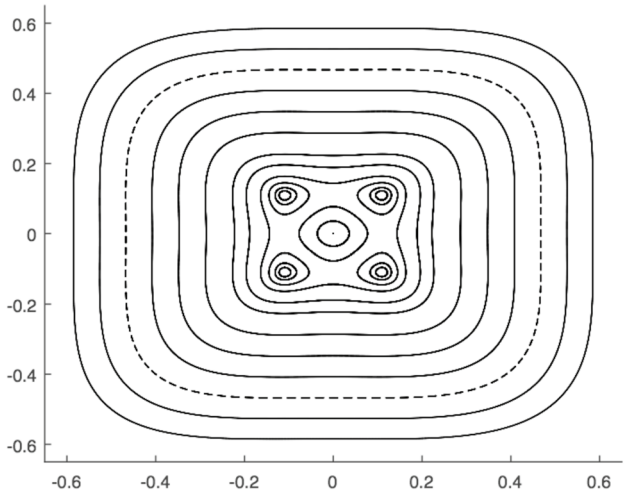

Fig. 4 The phase-portrait of (14) for $f(x) = x - \sin x$, and $R = 1$, while $\theta = \frac{\pi}{2} + 0.001$. It is remarkable to see that periodic solution with a period of four times the period of the kicked is actually achieved when one detune away from the 1:4-resonance

to see that the first function can be achieved from the Taylor expansion of the second function by truncation up to order 5.

The effect of detuning

Lastly, we are considering the effect of a small perturbation in θ, i.e.: $\theta = \frac{1}{2}\pi + 0.01$. This type of perturbation (where we perturbed the rotation angle) is usually called detuning. It is interesting to see that when θ is near $\frac{1}{2}\pi$ we have observed the existence of period-4 points in the neighborhood of the origin.

Thus, we note that in the case where $\theta = \frac{\pi}{2}$, although the linear dynamics (mapping (9) with $R = 0$) consists of period-4 points, it seems that none of these points survive the perturbation ($R \neq 0$) we are considering in this paper. Instead of period-4 point, we have observed the existence of other periodic points. Period-4 points have been observed in the case where we detuned the angle from $\frac{\pi}{2}$. See Fig. 4. This is a subject of future investigation.

Acknowledgements JMT thanks Prof. W.T. van Horssen (Technical University Delft, the Netherlands) , Prof. G.R.W. Quispel and Prof. P. H. van der Kamp (La Trobe University, Melbourne, Australia) for their hospitality during his visits to both universities during the execution of this research.

Funding This research is supported by Riset P3MI 2017, Institut Teknologi Bandung, Indonesia.

Compliance with ethical standards

Conflict of Interest The authors declare that they have no conflict of interest.

References

1. Arrowsmith DK, Place CM, Place C et al (1990) An introduction to dynamical systems. Cambridge University Press, Cambridge
2. Hale JK, Koçak H (2012) Dynamics and bifurcations, vol 3. Springer, Berlin
3. Hénon M (1969) Numerical study of quadratic area-preserving mappings. Q Appl Math 27:291–312
4. Siegel CL, Moser JK (2012) Lectures on celestial mechanics. Springer, Berlin
5. Möser J (1962) On invariant curves of area-preserving mappings of an annulus. Nachr Akad Wiss Göttingen II:1–20
6. Möser J (2016) Stable and random motions in dynamical systems: with special emphasis on celestial mechanics (AM-77). Princeton University Press, Princeton
7. Verhulst F (2012) Extension of poincare's program for integrability, chaos and bifurcations. Chaot Model Simul 1:3–16
8. Gaeta G (2002) Poincaré normal and renormalized forms. Acta Appl Math 70(1–3):113–131
9. Sanders JA, Verhulst F, Murdock J (2007) Averaging methods in nonlinear dynamical systems. Applied mathematical sciences, vol 59. Springer, New York
10. Rink B, Tuwankotta T (2005) Stability in hamiltonian systems. In: Montaldi J, Ratiu T (eds) Geometric mechanics and symmetry:

the Peyresq lectures. LMS lecture note series 306. Cambridge University Press, pp 1–22
11. Tuwankotta J, Verhulst F (2001) Symmetry and resonance in hamiltonian systems. SIAM J Appl Math 61(4):1369–1385
12. Tuwankotta JM, Quispel G (2003) Geometric numerical integration applied to the elastic pendulum at higher-order resonance. J Comput Appl Math 154(1):229–242
13. Lorenz EN (1963) Deterministic nonperiodic flow. J Atmos Sci 20(2):130–141
14. Zaslavskii G, Zakharov MY, Sagdeev R, Usikov D, Chernikov A (1986) Stochastic web and diffusion of particles in a magnetic field. Sov Phys JETP 64(2):294–303
15. Hoveijn I (1992) Symplectic reversible maps, tiles and chaos. Chaos Solitons Fractals 2(1):81–90
16. Lowenstein J (2005) Sticky orbits of a kicked harmonic oscillator. In: Journal of Physics: conference series, vol 7. IOP Publishing, p 68
17. Kells G, Twamley J, Heffernan D (2004) Dynamical properties of the delta-kicked harmonic oscillator. Phys Rev E 70(1):015203
18. Fromhold T, Krokhin A, Tench C, Bujkiewicz S, Wilkinson P, Sheard F, Eaves L (2001) Effects of stochastic webs on chaotic electron transport in semiconductor superlattices. Phys Rev Lett 87(4):046803
19. Gardiner SA, Cirac J, Zoller P (1997) Quantum chaos in an ion trap: the delta-kicked harmonic oscillator. Phys Rev Lett 79(24):4790
20. Billam T, Gardiner S (2009) Quantum resonances in an atom-optical δ-kicked harmonic oscillator. Phys Rev A 80(2):023414
21. Lemos GB, Gomes RM, Walborn SP, Ribeiro PHS, Toscano F (2012) Experimental observation of quantum chaos in a beam of light. Nat Commun 3:1211
22. Levi B, Georgeot B, Shepelyansky DL (2003) Quantum computing of quantum chaos in the kicked rotator model. Phys Rev E 67(4):046220
23. Mukhopadhyay S, Demircioglu B, Chatterjee A (2011) Quantum dynamics of a nonlinear kicked oscillator. Nonlinear Dyn Syst Theory 11(2):173–182
24. Reynoso MP, Vázquez PL, Gorin T (2017) Quantum kicked harmonic oscillator in contact with a heat bath. Phys Rev A 95(2):022118
25. You-Yang X (2013) Interference of quantum chaotic systems in phase space. Commun Theor Phys 60(4):453
26. Mudde RF, Jansz SG (2003) Influence of damping on the delta-kicked harmonic oscillator with heaviside kick. Phys D Nonlinear Phenom 179(1–2):1–17
27. Viana RL, Batista AM (1998) Synchronization of coupled kicked limit cycle systems. Chaos Solitons Fractals 9(12):1931–1944